Chapter 11
Testing Wooden Elements for the Building of Domes

11.1 Introduction

The selection and choice of wood for the building of domes is a difficult task. Neither objective criteria for the choice of a wood species nor the best planks for the building of dome structures have been developed. Globally, the application of various wood species, most often the local ones, is noticed, and the choice of the best planks follows manually. The choice of wood species most useful for the building of structures on the basis of a tradition and the choice of planks on the basis of visual methods is worth supplementing with the physical testing methods taking into account the conditions and the operational life of constructions. It is suggested in this chapter **to supplement the recognition of the usefulness of wood for the building of domes on the basis of the free vibration measurement**.

The wood used for the building of prestigious wooden domes have to exhibit good physical properties, including strength parameters to ensure the required durability of the construction. Therefore, an effective selection of wood is necessary so as to choose from the mass of the best planks for the most strenuous elements of the construction, and to use planks of a worse quality in secondary elements, or to reject them.

In the daily practice the choice of wood for construction follows on the basis of a visual inspection. For instance, the Japanese Miyazaki Prefectural Wood Utilization Research Center responsible for the production of the Konohana Dome in the town of Miyazaki in 2002 (described in Chap. 8) made the choice of the best planks according to the measurement of the spacing between the fibres in the wood section [1]. Shown in Fig. 11.1 is the section glued from planks cut out from 45-year-old sugi trees. Planks were so selected that the spacing between rings were included within the range of 4–14 mm.

Demonstrated in Fig. 11.2 is the testing consisting in the sending of acoustic waves in the upper zone of the ceiling beam. Two sensors are installed on the

B. Misztal, *Wooden Domes*, https://doi.org/10.1007/978-3-319-65741-7_11

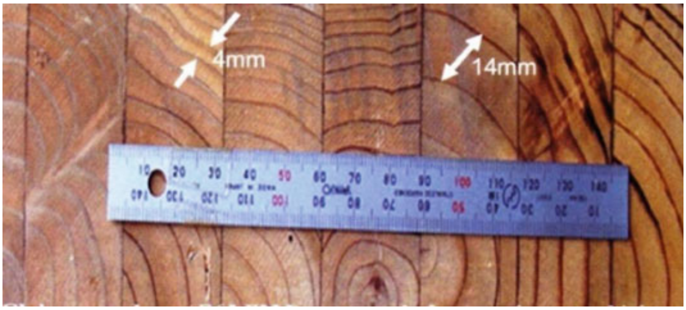

Fig. 11.1 Planks selected on the basis of the spacing criterion between rings [1] by Yutaka Iimura (2002)

section of the wood being tested. With a hammer blow in one of the sensors the acoustic wave flowing to the next sensor is excited. The measurement of the wave flow resistance multiplied by the coefficient adopted in the measurement method is a conventional value of the modulus of direct elasticity of the material. It is assumed in this method that the acoustic wave flow rate also allows to make a comparative assessment of damages to the specimen being tested.

Shown in Fig. 11.2 is the FAKOPP Microsecond Timer device. The formula for the coefficient **v** suggested in [2]: v [m/s] = 1000 × l_a/FAKOPP [μs] − 4.5,

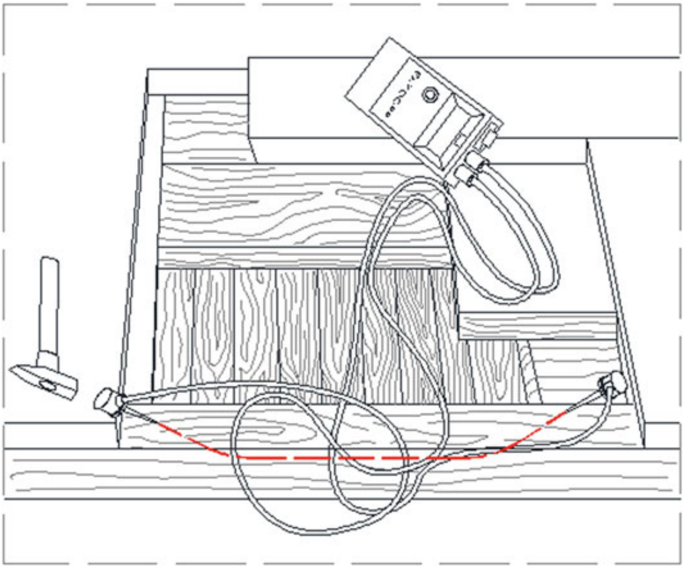

Fig. 11.2 Testing schematic of the beam through the measurement of the acoustic wave flow rate in wood between the sensors. The wave flow path is marked with a red dotted line

where "*v*"—wave flow rate [m/s], l_a—spacing between the measurement sensors as measured in [mm]. "ν" is the coefficient read on the device demonstrated in Fig. 11.2.

In this method it is recommended to calculate the dynamic module of direct elasticity (Ed) at the known wood density of the beam being tested "**ρ**" from the formula:

$$E_d = \nu^2 \times \rho.$$

where: ***v***—coefficient read out on the device, "***ρ***"—density of wood being tested.

As known from the paper [3], the flow rate of the acoustic wave depends mainly on the length of the fibres of the wood being tested. It does not depend on the wood density. The properties of the structural wood depend not only on the length of its fibres, as demonstrated in Chap. 9. The properties of wood depend on many factors, among others, on the properties of the matrix in which wood fibres are inundated and the quality of their fastening in the said matrix.

The methods presented allow, in the opinion of the author, to make local measurements and a local assessment of the individual features of the wood sample being tested. **Most often, beside the local data, the global information about the technical state of the element and the value of, e.g., of the modulus of elasticity *E* for a wooden beam or post, is required. To this aim, the author recommends short dynamic tests for the selection, evaluation and determination of the stiffness of elements, as well as the modulus of direct elasticity E from various wood species**.

Many authors were dealing with the issues of dynamics of visco-elastic structures. Among others, Nowacki W. in his monograph [4] (1972) specifies the solutions related to the dynamics of some visco-elastic systems and the propagation of visco-elastic waves. The author presented the mathematical fundamentals for the dynamics of linear visco-elastic constructions.

The work tasks of the loss of the stability of visco-elastic compressed bars are formulated and resolved by Kowal Z. in his papers [5] (1966) and [6] (2005) and other papers. In the paper [5] (1966), he resolves the issue of the buckling of a compressed bar in a visco-elastic medium. The author analyses the vibration: of a visco-elastic and a stiff beam on the supports: viscous, visco-elastic and stiff. He determines the dynamic coefficients to determine the maximum vibration amplitude and the maximum forces within the system. Kowal Z. describes the free vibration measurement method in his paper [7] (1983) for a practical application. It was used for the comparative detection of girders damaged in a flat roof having the construction from prestressed concrete girders. Upon excitation up to vibration of successive girders, the frequency of their free vibration was measured. The lowest frequencies were exhibited by damaged girders of a lower stiffness. This allowed to conclude about the need of their replacement or strengthening. This method is also suitable to detect damaged planks and wooden beams.

Langer J. in his paper [8] (1980) on the subject of the vibration of flat bar systems as well as the vibration of solids on an elastic substrate called attention that the free vibration of constructional systems of a low damping are described in practice by an equation derived for the Kelvin-Voigt model. The author stated, however, that the Kelvin-Voight model does not describe sufficiently the statics and dynamics of building constructions. Like Kowal Z., he demonstrates in his numerous publications that in the Kelvin-Voigt model there is no element to reflect the immediate deflection of a construction under the influence of loads, and this model used so far yields increases values of forces and a decreased assessment of the shifts of a construction. On the other hand, the Maxwell model shows increased amplitudes and reduced forces within the system.

The testing of the free vibration allows the comparative analysis of the vibration parameters of construction elements. On the basis of the comparison of the measured circular speeds of the own free vibration $\boldsymbol{\alpha}$ of similar beams there is a possibility to detect dry and wet beams, and to differentiate damaged beams from undamaged beams. To this aim, the logarithmic vibration damping decrements $\boldsymbol{\Delta}$ on the basis of dimensional damping coefficients $\boldsymbol{\rho}$ should be calculated. For the first time, the author recommended the dynamic testing in the diagnostics of wooden constructions in her paper [9] (2004).

The authors Kokociński W., Poliszko S., J. Raczkowski [10] (1982) described the creep of wood under the conditions of a dynamic extortion. The authors do not define the practical conclusions resulting from the dynamic testing. They specify that:

1. the dynamic extortion activates the process of the static creep of wood,
2. the creep speed at low cycles (3 cycles per minute) is comparable to that of static creep,
3. at higher frequencies >30 cycles per minute the creep speed is higher than that of static creep,
4. as the amplitude of translocations from applied load rises, the difference between the static creep and the vibro-creep increases,
5. according to [10], the static and dynamic forced distortions are subject to a description using the same function of creep.

They called attention to the missing dynamic testing of wooden structural elements. The authors have demonstrated that: (1) in the case of statically loaded wooden constructions, the introduction of vibrational load produces enhanced distortions and creeping translocations, (2) the wood creep model changes under the influence of moisture variations.

Jakowluk A. in his paper [11] (1993) examined the vibro-creep of samples from materials with a plastic stop (metals). The author describes the impact of harmonic vibration on the creeping process. The samples of materials were loaded statically and subjected to a harmonic load. The author defines the vibro-creep as the process of the impact of a dynamic load, of a low stress amplitude A_σ in metals, on the process of static creep. He assumes that vibration does not produce the fatigue of a material, but jointly with the action of a static stress brings about a creep leading to destruction.

The hypothesis about the use of the dynamic testing to the calculation of the modulus of elasticity of wood and the evaluation of the technical state of wood was formulated for the first time in the experimental works by Misztal B. [9] (2004), [12] (2008), [13] 2010.

These hypotheses were presented in the testing of models from wood and wood-based materials, as described in this chapter and Chap. 12 **of this publication**.

11.2 Dynamic Testing Oriented Towards the Choice and Selection of Wood for the Construction of Domes

It is suggested to measure the free vibration parameters of wooden, plank-supporting elements, instead of the commonly applied long-term testing or visual inspection as discussed in the preface. This will allow the verification whether the testing of the free variation of wooden elements is suitable for the selection of wood for the construction for domes.

The recognition of the features of wood on the basis of a dynamic testing, yielding clear results, instead of visual inspections, long-term testing or the measurement of flow speed of acoustic waves was suggested.

The measurement and calculation method of the free vibration parameters following the examples of dry and wet models of beams from wood: pine, spruce, larch and oak is demonstrated in this chapter. The aim of the testing was to determine the degree of the suitability of various wood species for the building of constructions, domes in particular.

The rate of the deflection reduction upon removal of the load was adopted as one of the criteria of the suitability of wood for the building of domes.

Models of dry and wet planks, of a 10 × 40 mm section, 1200 mm long were prepared for the testing. The models were made from pine, spruce, larch and oak wood. Before the experiment, the planks were weighed in a dry-air state. After the dynamic testing of dry planks, they were soaked in water for 24 h. After the wetting, the planks were re-weighed, and their moisture by weight was calculated. Planks loaded with a fixed mass of 250 g, cantilever-wise, like in the figure, were set in a vibrating motion. The extortive load was applied at the end of the support perpendicularly to the plane of the lower stiffness of the beam (Fig. 11.3).

The frequency $\boldsymbol{n}$ and the damping $\boldsymbol{\rho}$ of the free vibration extorted by a pulse via the load P = 250.0 g suspended on a threat at the end of the support was tested. The vibration was extorted through the cutting of the load-maintaining thread. After the wetting in water, the testing of the impact of the wetting of wooden beams on the frequency $\boldsymbol{n}$ and the damping $\boldsymbol{\rho}$ of free vibration and the creep of beams was carried out.

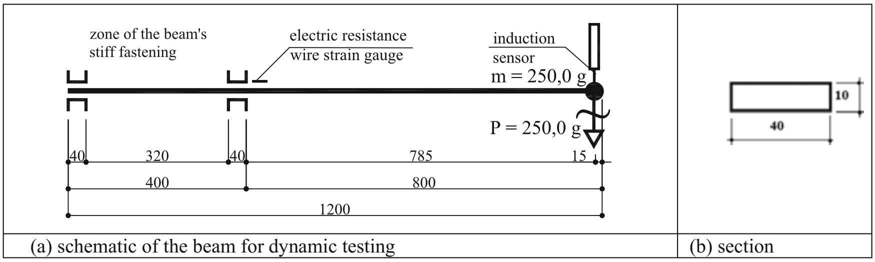

Fig. 11.3 Model of the beams being tested

In all cases, the damped free vibration measured, regardless of the wood species, was well described by the function (11.1) [14]:

$$y_t = y_0 e^{-\rho t} \cos(t\omega + \varphi) \Rightarrow y_t = y_0 e^{-\rho t} \cos\left(t\sqrt{\alpha^2 - \rho^2} + \varphi\right), \qquad (11.1)$$

where:

α circular frequency of own vibration,
ρ dimensional vibration damping
φ phase displacement

$$\omega = \sqrt{\alpha^2 - \rho^2} \quad \text{circular frequency of damped vibration} \qquad (11.2)$$

Placed below are the vibrating motion parameters as measured on the models from dry and wet planks and as assessed according to the formulae as follows:

– vibration frequency:

$$n = \frac{1}{T}\left[\frac{1}{s}\right], \qquad (11.3)$$

– vibration period T measured in [s],
– circular speed ω of damped vibration speed was calculated from the formula:

$$\omega = 2\pi n \qquad (11.4)$$

– logarithmic damping decrement Δ was calculated from the formula:

$$\Delta = \ln\frac{A_i}{A_{i+1}} = \ln\frac{e^{-\rho t}}{e^{-\rho(t+T)}} = \rho T \qquad (11.5)$$

– where A_i, A_{i+1} are successive vibration amplitudes
– dimensional damping coefficient ρ totals:

$$\rho = \Delta/T[1/s]. \tag{11.6}$$

For each of dry and wet beams the vibrating motion parameters were calculated: for dry models with an index "s": T_s, y_0, ρ_s, n_s, $\boldsymbol{\omega_s}$, Δ_s, and for wet models with an index "m": T_m, y_0, ρ_m, n_m, ω_m, Δ_m, where: n—vibration frequency, T—vibration period, ρ—damping coefficient, Δ—logarithmic damping decrement.

The vibration chart of the model from a dry pine-wood plank is presented in Fig. 11.4. This is an exemplary chart of the free damped vibration of a pine-wood plank during 10 s of the testing (Table 11.1).

The vibration chart of a model from a pine wood plank is presented in Fig. 11.5. This is an exemplary chart of the damped vibration of a pine wood plank of a 56.62% moisture by weight, during 10 s of the testing (Table 11.2).

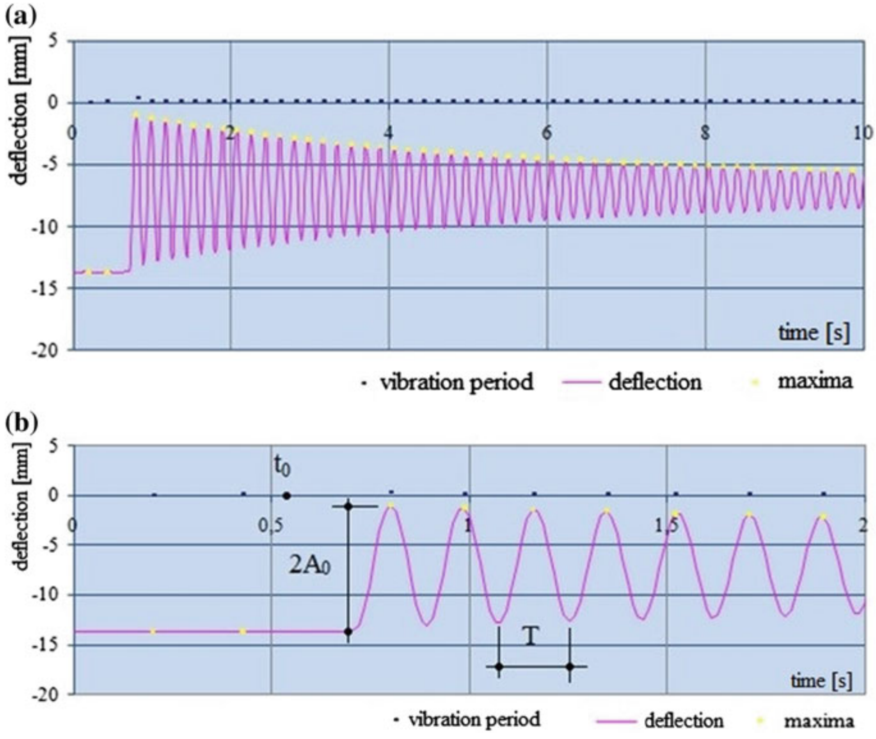

Fig. 11.4 Vibration chart **a** of the pine-wood model in dry-air state during 10 s of the testing, **b** during the first 2 s of the testing

Table 11.1 Parameters of the vibrating motion of the model tested according to Fig. 11.3 from pine wood in a dry-air state, burdened with a concentrated mass at the end

T_s [s]	t_0 [s]	y_0 [mm]	ρ_s [1/s]	$n_s = 1/T$ [1/s]	ω_s [1/s]	φ [°]	Δ_s
0.186	0.5733	13.68	0.14	5.38	33.8	11.15	0.026

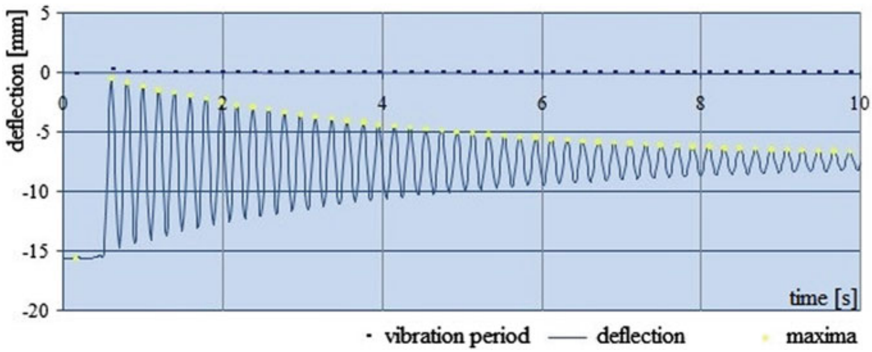

Fig. 11.5 Record of the vibrating motion of a model from pine wood burdened at the end during 10 s

Table 11.2 Vibrating motion parameters of a model according to Fig. 11.3 from wet pine wood of a 56.62% moisture, burdened with a concentrated mass at the end

T_m [s]	t_0 [s]	y_0 [mm]	ρ_m [1/s]	$n_m = 1/T$ [1/s]	ω_m [1/s]	φ [°]	Δ_m
0.1117	0.506	15.57	0.2411	5.076	31.811	3.21	0.04112

Table 11.3 The vibrating motion parameters of a model according to Fig. 11.3 from spruce wood in a dry-air state, burdened with a concentrated mass at the end

T_s [s]	t_0 [s]	y_0 [mm]	ρ_s [1/s]	$n_s = 1/T$ [1/s]	ω_s [1/s]	φ [°]	Δ_s
0.17	0.2667	13.99	0.172429	5.8823	35.35994	−3.49754	0.029313

Placed in Table 11.3 are the parameters of the vibrating motion T_s, y_0, ρ_s, n_s, $\boldsymbol{\omega_s}$, Δ_s and in Fig. 11.6 an exemplary chart of the damped free vibration of a spruce wood plank model in a dry-air state.

Placed in Table 11.4 are the vibrating motion parameters as well as in Fig. 11.7 an exemplary chart of the damped free vibration of a spruce wood plank model of a 34.92% moisture content.

Placed in Table 11.5 are the vibrating motion parameters T_s, y_0, ρ_s, n_s, $\boldsymbol{\omega_s}$, Δ_s as well as in Fig. 11.8 an exemplary chart of the damped free vibration of a larch wood plank model in a dry-air state.

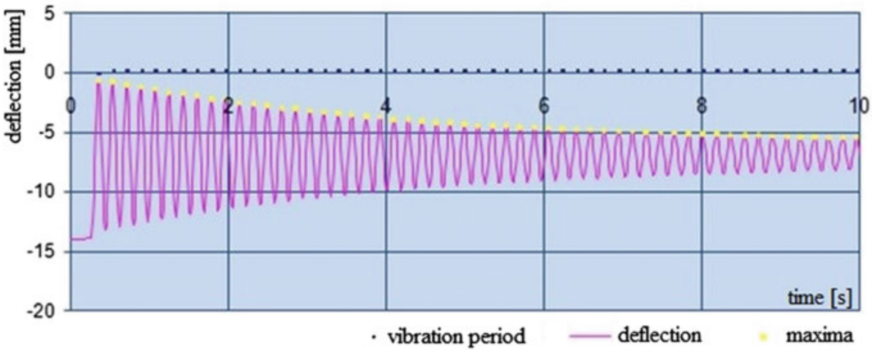

Fig. 11.6 Record of the vibrating motion of a model from spruce wood burdened at the end during 10 s

Table 11.4 The vibrating motion parameters of a model according to Fig. 11.3 from wet spruce wood of a 34.92% moisture content, burdened with a concentrated mass at the end

T_m [s]	t_0 [s]	y_0 [mm]	ρ_m [1/s]	$n_m = 1/T$ [1/s]	ω_m [1/s]	φ [°]	Δ_m
0.187	0.4667	14.85	0.263616	5.3475	34.11056	−3.51436	0.0493

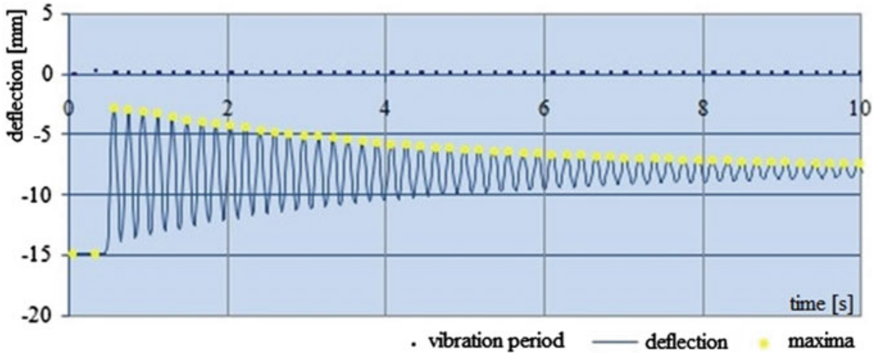

Fig. 11.7 Record of the vibrating motion of a model from wet spruce wood burdened at the end during 10 s

Table 11.5 Vibrating motion parameters of a model according to Fig. 11.3 from larch wood in a dry-air state, burdened with a concentrated mass at the end

T_s [s]	t_0 [s]	y_0 [mm]	ρ_s [1/s]	$n_s = 1/T$ [1/s]	ω_s [1/s]	φ [°]	Δ_s
0.21	0.72	18.76	0.148506	4.7619	30.01375	21.70679	0.0312

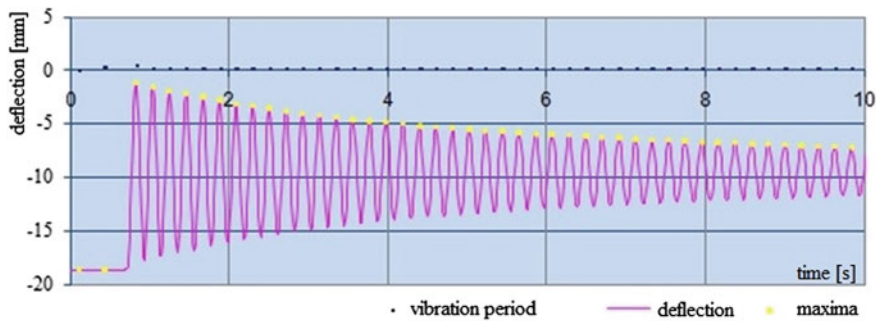

Fig. 11.8 Record of the vibrating motion of a model from larch wood in a dry-air state during the first 10 s of the testing

Table 11.6 The vibrating motion parameters of a model from wet larch wood of a 25.93% moisture content, burdened with a concentrated mass at the end

T_m [s]	t_0 [s]	y_0 [mm]	ρ_m [1/s]	$n_m = 1/T$ [1/s]	ω_m [1/s]	φ [°]	Δ_m
0.22	0.4533	21.16	0.256217	4.54	28.5664	9.524647	0.0564

Placed in Table 11.6 are the vibrating motion parameters of a larch wood plank of a 25.93% moisture content by weight. Figure 11.9 presents an exemplary chart of damped vibration during the first 10 s of the testing.

Placed in Table 11.7 are the vibrating movement parameters T_s, y_0, ρ_s, n_s, $\boldsymbol{\omega_s}$, Δ_s as well as in Fig. 11.10 an exemplary chart of the damped free vibration of an oak wood plank model in a dry-air state. Figure 11.10 demonstrates an exemplary chart of damped vibration during the first 10 s of the testing.

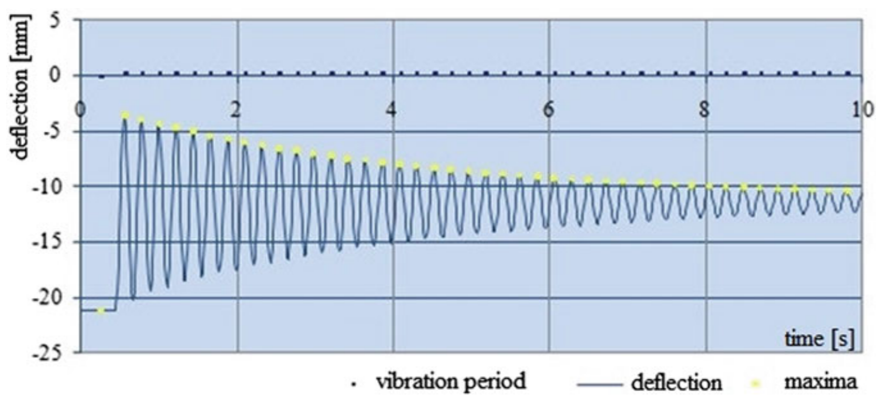

Fig. 11.9 Record of the vibrating movement of a model from wet larch wood during the first 10 s of the testing

Table 11.7 The vibrating motion parameters of a model tested according to Fig. 11.3 from oak wood in a dry-air state, burdened with a concentrated mass at the end

T_s [s]	t_0 [s]	y_0 [mm]	ρ_s [1/s]	$n_s = 1/T$ [1/s]	ω_s [1/s]	φ [°]	Δ_s
0.253	0.11067	25.77	0.1673	3.953	24.835	2.251	0.0423

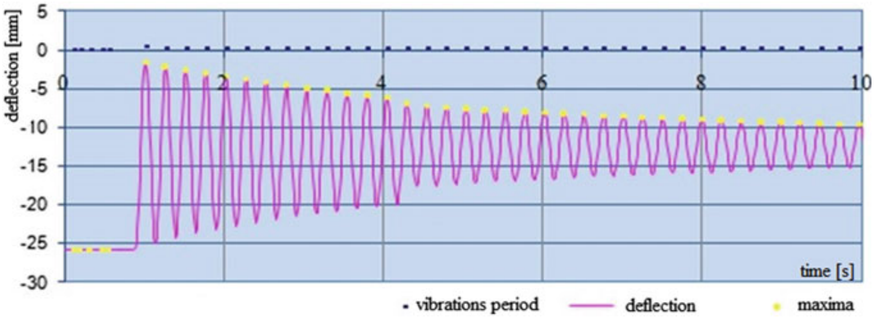

Fig. 11.10 Vibration chart of a model from oak wood in a dry-air state during the first 10 s of the testing

Placed in Table 11.8 are the vibrating motion parameters of an oak wood plank of a 23.00% moisture content. Figure 11.11 demonstrates the damped vibration charts of a wet oak wood plank during the first 10 s of the testing.

Table 11.9 demonstrates the impact of the increase in moisture content of beams from pine wood on the free vibration parameters of the models. Pine wood was selected as a representative of coniferous construction wood species, oak wood as a representative of deciduous wood species.

Presented in Table 11.10 are the ratios of the vibration parameters of wet models versus the vibration parameters of dry models characterizing the impact of the increase in moisture content on beams from oak wood. The determination of the vibration parameters is like in Table 11.9.

The models of small beams from wood were also subjected to a testing consisting in the six-fold pulse excitation with a force of 250.0 g, (each model separately) according to the scheme as in Fig. 11.3. For each model, after the testing, the residual deflection was observed. The total deflection upon completion of six excitation trials of one model was adopted as residual deflection. After a variable time for the given model, the deflection was decreased down to a value that did not decrease any more (Table 11.11). Such a deflection was called a permanent deflection.

Table 11.8 The vibrating motion parameters of a model tested according to Fig. 11.3 from wet oak wood of a 23.00% moisture content burdened with a concentrated mass at the end

T_m [s]	t_0 [s]	y_0 [mm]	ρ_m [1/s]	$n_m = 1/T$ [1/s]	ω_m [1/s]	φ [°]	Δ_m
0.267	0.6	30.98	0.236	3.745	23.5325	15.876	0.063

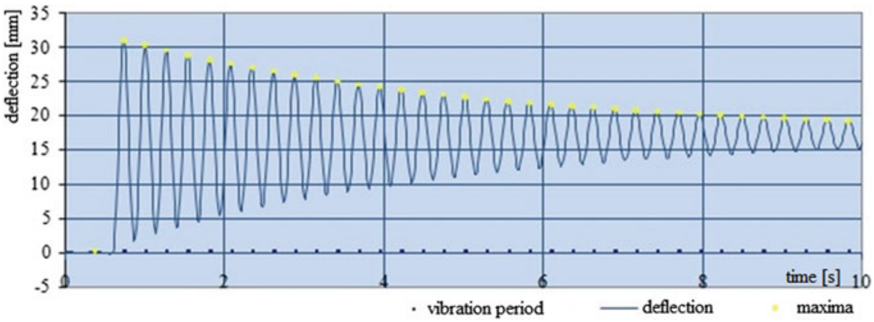

Fig. 11.11 Record of the vibrating motion of a model from wet oak wood burdened at the end during 10 s

Table 11.9 Ratios of the free vibration parameters of wet pine wood versus dry pine wood

Pine wood						
1	2	3	4	5	6	7
$\frac{n_m}{n_s}$	$\frac{T_m}{T_s}$	$\frac{\rho_m}{\rho_s}$	$\frac{\Delta_m}{\Delta_s}$	α_s	α_m	$\frac{\alpha_m}{\alpha_s}$
0.9435	1.0511	1.785	1.822	33.8[1/s]	31.8[1/s]	0.94

where
n_m—vibration frequency of a wet plank
n_s—vibration frequency of a dry plank
T_m, T_s—vibration period of a wet plank and a dry plank
ρ_m, ρ_s—vibration damping coefficient of a wet plank and a dry plank
Δ_m, Δ_s—logarithmic damping decrement of a wet plank and a dry plank
α_m, α_s—circular speed of the undamped free vibration of a wet plank and a dry plank, $\alpha = \sqrt{\omega^2 + \rho^2}$

Table 11.10 Comparison of the free vibration parameters of a dry oak wood plank versus a wet oak wood plank

Oak Wood						
1	2	3	4	5	6	7
$\frac{n_m}{n_s}$	$\frac{T_m}{T_s}$	$\frac{\rho_m}{\rho_s}$	$\frac{\Delta_m}{\Delta_s}$	$\boldsymbol{\alpha_s}$	$\boldsymbol{\alpha_m}$	$\frac{\alpha_m}{\alpha_s}$
0.947	1.0553	1.41	1.488	24.836 [1/s]	23.534 [1/s]	0.9476

The models from wood subjected to the six-fold pulse excitation during several dozens of minutes exhibited such residual deflections like after a long-term static testing. The pulse-excited vibration allowed a preliminary discrimination of visco-elastic models of various wood species during a dozen or so minutes, and several dozens of months, like in the case of the long-term testing for static creep.

Table 11.11 Comparison of deflections and vibration periods of four wood species after six excitation cycles up to vibration using a 250.0 g mass

Wood species	Residual deflection of the support's end after 6 excitations using a 250 gf force	Permanent deflection of the support's end	Dry beams	Wet beams
			Vibration period	Vibration period
1	2 [mm]	3 [mm]	4 [s]	5 [s]
Pine	0.29	0.05	0.07	0.18
Spruce	0.13	0.02	0.07	0.17
Larch	0.39	0.07	0.074	0.21
Oak	2.93	2.01	0.106	0.253

The least residual deflection after 6 cycles of pulse-excited vibration is exhibited by coniferous trees' species. Among the coniferous species, the highest permanent deflection is demonstrated by larch wood.

The lowest vibration period is owned by pine wood, the highest vibration period by oak wood. The vibration period depends on the mass of a construction. The significant difference in the vibration periods specified in columns 4 and 5 of Table 11.11 results from a different mass of dry planks and wet planks. To a low degree, it follows from a various vibration damping. It has also been noticed that each element tested differed insignificantly by the free vibration period. **The vibration period within one trial of each of the planks tested was a fixed value**.

The models from wood were also tested in order to assess the moduli of direct elasticity E_s in a dry-air state and after a 24-h soaking in water. The description of the testing and the statement of the results are specified in Sect. 11.3.

11.3 Dynamic Testing Results Oriented Towards the Determination of the Modulus of Direct Elasticity E of Wood

On the basis of the dynamic testing conducted on a test stand presented in Sect. 11.2 according to the schematic shown in Fig. 11.3 it is recommended to determine the frequency $\boldsymbol{n}$ and the damping $\boldsymbol{\rho}$ of free vibration in order to assess the modulus of direct elasticity of wood. The vibrating motion parameters $\boldsymbol{T}$, $\boldsymbol{\rho}$ $\boldsymbol{\omega}$, $\boldsymbol{\Delta}$, shown in Tables 11.1, 11.2, 11.3, 11.4, 11.5, 11.6, 11.7, and 11.8 were determined on the basis of the numerical measurement results using EXCEL spreadsheets. Vibration was excited through the cutting of a thread maintaining a load of P = 250.0 g suspended at the end of the support. After soaking in water, the testing of the impact of the wetting of wooden beams on the frequency $\boldsymbol{n}$ and the damping $\boldsymbol{\rho}$ of free vibration and the modulus of direct elasticity of beams was performed.

The testing of the models of pine, spruce and larch wood planks representing coniferous species of construction wood and that of an oak wood plank, as the representative of deciduous species was carried out. The testing was done on dry models and after a 24-h soaking in water.

In all cases the damped free vibration, as described by the function (11.1) are discussed in Sect. 11.2. For each of the beams the free vibration parameters were calculated using the formulae (11.2) through (11.6) and compiled in Tables 11.1 through 11.8. The calculated modulus of elasticity $\boldsymbol{E}$ is compiled in Tables 11.12 and 11.13, in columns: 9 and 10, developed in this chapter.

Kowal Z. specified in his paper [14] (1966) the relationships between the stiffness $\boldsymbol{K}$, the mass—$\boldsymbol{m_z}$, the vibration speed $\boldsymbol{\omega}$ and the damping $\boldsymbol{\rho}$. The dependence was derived from the equation of the motion of a visco-elastic body written in form of the formula (11.7):

$$m_z \overset{**}{y} + K_\eta \overset{*}{y} + Ky = 0 \tag{11.7}$$

$$m_z \overset{**}{y} + K_\eta \overset{*}{y} + Ky = 0/m_z \tag{11.8}$$

$$\overset{**}{y} + \frac{K_\eta}{m_z} \overset{*}{y} + \frac{K}{m_z} y = 0 \tag{11.9}$$

$$\alpha^2 = \frac{K}{m_z} \tag{11.10}$$

$$\rho^2 = \frac{K_\eta}{m_z} \tag{11.11}$$

$$\alpha^2 = \omega^2 + \rho^2 \tag{11.12}$$

In the absence of damping, there is the equation of the free vibration of a spring:

$$m_z \overset{**}{y} + Ky = 0/m_z \tag{11.13}$$

The assessment of the stiffness $K = \alpha^2 m_z$ is understated since the actual stiffness will be slightly higher as damping occurs:

$$\omega^2 = \alpha^2 - \rho^2 \tag{11.14}$$

In the elastic system of one degree of freedom the relationship occurs:

$$K\,y = P \tag{11.15}$$

Table 11.12 Comparative compilation of the modulus of direct elasticity E of the tested in a dry-air state

Dynamic parameters in a dry-air state tested according to Fig. 11.3						m_z [g]	$K = m_z\alpha_s^2$ [g/s^2]	E_s of models in dry-air state [GPa]	E as per the standard [GPa]
Material	Model's mass [g]	Evenly distributed mass [g/m]	ρ_s	ω_s	Own vibration				
			ρ_s^2 [1/s]	ω_s^2 [1/s]	$\alpha_s^2 = \rho_s^2 + \omega_s^2$ [1/s^2]				
1	2	3	4	5	6	7	8	9	10
Pine wood	260.70	178.15	0.14	33.80		285.498	326,170.1	**17.98**	**11–14**
			0.0196	1142.44	1142.46				
Spruce wood	224.58	153.46	0.1724	36.3168		280.578	370,065.5	**20.40**	
			0.0297	1318.91	1318.94				
Larch wood	267.60	182.86	0.1485	30.01375		286.437	258,035.6	**14.23**	
			0.0220	900.825	900.847				
Oak wood	314.42	214.85	0.1673	24.835		292.811	180,607.3	**9.96**	**No data**
			0.028	616.777	616.805				

Table 11.13 Comparative compilation of the moduli of direct elasticity E_m of the tested models after a 24-h soaking in water

Dynamic parameters of wet models tested according to Fig. 11.3						m_z [g]	$K = m_z\ \alpha_s^2$ [g/s^2]	Moisture content [GPa]	E_m [GPa]	Reduction of E [%]
Material	Model's mass [g]	Evenly distributed mass [g/m]	ρ_m / ρ_m^2 [1/s]	ω_m / ω_m^2 [1/s]	$\alpha_m^2 = \rho_m^2 + \omega_m^2$ [1/s^2]					
1	2	3	4	5	6	7	8	9	10	11
Pine wood	408.30	279.00	0.2411	31.811		305.594	309,260.05	56.6	**17.05**	**5.0**
			0.0581	1011.94	1011.998					
Spruce wood	308.52	210.82	0.2636	33.6		292.008	329,685.65	34.9	**18.18**	**10.9**
			0.0695	1128.96	1129.0295					
Larch wood	337.00	230.28	0.2562	28.5664		295.886	241,474.01	25.9	**13.31**	**6.5**
			0.06565	816.04	816.106					
Oak wood	386.70	264.23	0.236	23.5325		302.650	167,618.73	23.0	**9.24**	**7.2**
			0.0557	553.78	553.836					

Disregarding the viscosity η due to the low impact of damping on the stiffness of an element from wood (Table 11.13) on vibration frequency, one may assess the local stiffness ***K*** of the bar directly from the formula:

$$K = m_z \alpha^2 \approx m_z \omega^2 \tag{11.16}$$

The moduli of elasticity ***E*** were assessed from the below-specified algorithm.

When calculating the reduced mass of the test models, the actual, effective local stiffness of the tested beams was counted. The elastic stiffness K_{ef}, associating the load with the shift, $\boldsymbol{K_{ef} = P/y}$, is related to the measured vibration speed $\boldsymbol{\omega}$ and the damping $\boldsymbol{\rho}$ with the formula from the paper [14].

$$\alpha^2 = \omega^2 + \rho^2 = \frac{K_{ef}}{m_{zr}} \tag{11.17}$$

where: **ω**—measured frequency of damped free vibration [radians], $\boldsymbol{\rho}$—measured damping of free vibration, **α**—frequency of own vibration (undamped) [radians].

The immediate shift under the load $P = m_{zr}\ g$ can be determined from the formula:

$$y_o = P/K_{ef} \tag{11.18}$$

where: $K_{ef} = m_{zr}\ \alpha^2$ effective stiffness of the beam as measured on the model.

The circular speed of undamped free vibration, required to assess the elastic stiffness of dry and wet planks, was calculated from the formula (11.12).

$$\alpha = \sqrt{\omega^2 + \rho^2}\,[1/s] \tag{11.19}$$

where: **α**—own vibration, $\boldsymbol{\omega}$—free vibration, $\boldsymbol{\rho}$—vibration damping.

The local stiffness ***K*** of the support model was assessed on the basis of the substitutive concentrated mass $\boldsymbol{m_z}$ at the end of the support, as well as the measurement of the support's free vibration measurement **α** from the formula (11.16).

The square of the free vibration frequency $\alpha^2 = \omega^2 + \rho^2$ calculated after the testing on models is placed in Tables 11.12 and 11.13 (column 6).

The substitutive concentrated mass m_z resulting from the own mass of the support (of the tested model) was calculated from the formula (11.20) according to [15]:

$$\mathrm{m_z} = 0.243\,\mathrm{ql} + 250 \tag{11.20}$$

where: *q*—measured weight per running metre of the support.

The stiffness ***K*** of the models determined from the relationship $K_{ef} = m_z \alpha^2$ is placed in Tables 11.12 and 11.13—column 7.

The relationship between the stiffness $\boldsymbol{K}$ and the load $\boldsymbol{P}$ has the form from the Eq. (11.15), therefore:

$$y = \frac{P}{K} \Rightarrow K = \frac{P}{y} \qquad (11.21)$$

The shift $\boldsymbol{y}$ was determined from the formula:

$$y = \frac{Pl^3}{3EJ} = \frac{P}{K} \qquad (11.22)$$

The modulus of direct elasticity **E** was obtained from Eq. (11.21):

$$E = \frac{Kl^3}{3J} \qquad (11.23)$$

According to Fig. 11.3, the length of the support l = (785 + 20 + 15) mm = 0.82 m was assumed for the calculations of $\boldsymbol{E}$.

In Tables 11.12 and 11.13 the measured vibration parameters and the calculated stiffness values $\boldsymbol{K}$ and the moduli of direct elasticity $\boldsymbol{E}$ are compiled. The stiffness values $\boldsymbol{K}$ and the moduli of elasticity $\boldsymbol{E}$ of the tested wood species from dry and wet models were compared. In column 9 of Table 11.12 the assessment of the moduli of elasticity $\boldsymbol{E_s}$ of the tested dry models are compiled. In column 10 of Table 11.13 the assessment of the moduli of elasticity $\boldsymbol{E_m}$ of the tested wet models are compiled. The moisture content by weight of the models is specified in column 9 of Table 11.13.

The columns of Tables 11.12 and 11.13 were numbered and the following data were placed therein: in column 1—name of the material from which the model was made, in column 2—the mass 1 of the model, in column 3—mass in [g/m] of the support, in column 4—dimensional damping $\boldsymbol{\rho}$, in column 5—square of free vibration frequency $\boldsymbol{\omega^2}$, in column 6—square of own vibration frequency $\boldsymbol{\alpha^2}$, in column 7—substitutive mass $\boldsymbol{m_z}$, in column 8—stiffness of the support $\boldsymbol{K}$, in column 9—modulus of elasticity of dry models $\boldsymbol{E_s}$, Table 11.12 in column 10—modulus of elasticity of wet models $\boldsymbol{E_m}$, Table 11.13 in column 11—percentage reduction $\boldsymbol{E_m}$ after a 24-h soaking in water after a 2-h soaking in water.

11.4 Conclusions

Presented in Figs. 11.4, 11.5, 11.6, 11.7, 11.8, 11.9, 11.10, and 11.11 are the charts of the damped free vibration of plank models: from pine, spruce, larch and oak wood during the first 10 s of the testing. The comparison of the vibration of dry and wet planks allowed to determine significant differences in the vibration damping. **For each species of dry and wet planks the rations were calculated and placed in Tables** 11.1, 11.2, 11.3, 11.4, 11.5, 11.6, 11.7, 11.8, 11.9, 11.10, 11.11, 11.12,

and 11.13: —free vibration frequency of a wet plank n_m versus dry plank n_s: n_m/n_s, —vibration periods of a wet plank T_m versus a dry plank T_s: T_m/T_s. —damping coefficients of a wet plank ρ_m versus a dry plank ρ_s: ρ_m/ρ_s, —logarithmic damping decrements of a wet plank Δ_m versus a dry plank Δ_s: Δ_m/Δ_s.

It is possible to classify qualitatively, on the basis of the vibration measurements, the usefulness of the wood of the tested models for the application in construction according to the listing: pine, spruce, larch, oak. The highest vibration frequency was exhibited by a spruce, pine wood, the lowest vibration frequency by an oak wood plank.

The following can be done on the basis of the vibration damping magnitude of wooden elements:

1. to detect mechanically or biologically damaged elements within the set of similar elements,
2. to assess the usefulness of elements from various wood species for the construction of wooden constructions,
3. to detect wetted elements,
4. to select the usefulness of the same timber from the same wood species for the building of structures, especially those of prestige.

It is known from the engineering practice that wetted elements from wood have a lower resistance to biological elements and in such elements the reduction of load capacity and of the stiffness of wooden elements in time may be expected. It follows from the testing that wooden beams, of an increased moisture content, have a lower own frequency $\boldsymbol{n}$ and a significantly higher damping $\boldsymbol{\rho}$. One may anticipate that the high damping within the group of similar elements indicates the wet elements most exposed to the destruction by biological corrosion.

The conclusions deriving from the dynamic testing demonstrated in the publication may be used:

(1) to compare the creep speed and relaxation speed in combined elements from various wood species,
(2) to assess the rheological models of wood on the basis of vibro-creep,
(3) to assess the impact of moisture content on the mechanical properties of wood.

The conventional selection of wood species and wooden elements useful for the building of domes on the basis of visual inspections and traditions is worth supplementing by a dynamic testing since **the deviations of the vibration frequency and the vibration damping from the expected values are a significant indicator of hidden defects of an element**.

It follows from the analysis of the damping on the frequency of undamped vibration of dry models from wood that the damping has no essential impact on the stiffness of dry-air models from wood. The local actual stiffness K may be securely determined on the basis of the square of damped free vibration measured $\boldsymbol{\alpha^2 \sim \omega^2}$ from the formula $\boldsymbol{K_{ef} = \omega^2 m_z}$. For wood the assessment error of the tested wood does not reach 1%.

The lowest reduction of the modulus of elasticity of wood due wetting may be adopted as a criterion of the usefulness of wood for a long-term operation.

It is possible to forecast, on the basis of the dynamic testing of elements made from dry and wet elements from wood, their physical properties, thus their usefulness for the application in construction. The dynamic testing can be used for various purposes, including, for instance, the selecting of planks for the building of constructions, especially prestigious facilities. The planks of a higher damping should be rejected, and those exhibiting higher vibration frequencies and a lower logarithmic damping decrement can be used when a higher durability of a construction is required.

The dynamic testing allows a quick comparative qualitative analysis of the physical properties of wood. They allow to assess the fitness of wood for the use in constructions just after a few minutes, and not after several days, or even years, as in the case of the long-term testing. They allow a better recognition of the features of the wood being analysed, like the applied visual inspection of planks.

It follows from the analysis of the free vibration of models from wood that **species of a greater usefulness for construction exhibited lower vibration periods, higher vibration frequencies, a lower damping and a lower logarithmic damping decrement**.

The following occurred in the wet wood models: (1) the beams' mass increased, (2) the creep rose, (3) the damping increased, (4) the modulus of elasticity ***E*** decreased.

It follows from the dynamic testing conducted that the information obtained therefrom about the properties of wood are more unambiguous than that obtained after a long static testing. The recognition of the properties of wood is more precise than that on made on the basis of the static testing. Therefore, in the next chapter, the usefulness of the dynamic testing for the recognition of the mechanical properties of wood-based materials has been verified.

A short dynamic testing may be recommended for the selection of wood for the building of dome structures as well as to determine damaged elements in the wooden structures already built.

References

1. Iimura Y. *Performance Ewaluation of the "Konohana Dome"built with fast-growing Sugi* WCTE 2008 czerwiec 2–5 2008 Miyazaki Japan.
2. Zielski A., Krąpiec M., *Dendrologia,* PWN, Warszawa 2004.
3. Marcinkowska A., Moliński W. *Wpływ gęstości drewna na propagacje fal ultradźwiękowych wzdłuż włókien.* Annals of Warsaw Agricultural University SGGW, Forestry and Wood Technology No 53, Warsaw 2003.
4. Nowacki W., *Dynamika budowli,* Arkady, Warszawa 1972.
5. Kowal Z. *Wyboczenie pełzające osiowo ściskanych prętów lepkosprężystych,* III Sympozjum PTMTS poświęcone reologii, referaty t. i, Wrocław 1966, s. 209–218.

6. Kowal Z. *The effect of transverse forces on creeping buckling of viscoelastic compressed columns.* Arch. of Civil and Mechanical Engineering. Vol. V, No 2/2005, s. 13–23.
7. Kowal Z., Sendkowski J., Walasek A., *Wykrywanie porównawczą metodą dynamiczną elementów zarysowanych populacji belek strunobetonowych,* Politechnika Rzeszowska, Mechanika z.5, Rzeszów 1983.
8. Langer J., *Dynamika budowli*, Wydawnictwo Politechniki Wrocławskiej, Wrocław 1980.
9. Misztal B., *Pomiary dynamiczne w diagnostyce stropów drewnianych* REMO 2004 r. XI Konferencja Naukowo Techniczna Problemy Remontowe w Budownictwie Ogólnym i Obiektach Zabytkowych, Wrocław Zamek Kliczków, 9–11 grudnia 2004.
10. Kokociński W., Poliszko S., Raczkowski J., *Pełzanie drewna w warunkach wymuszenia dynamicznego*, Reologia drewna i konstrukcji drewnianych – Sympozjum Akademii Rolniczej w Poznaniu, materiały, Zielonka 21–22 października 1982.
11. Jakowluk A. *Procesy pełzania i zmęczenia w materiałach,* WNT, Warszawa 1993.
12. Misztal B., *Comparison of the Vibration Frequency and Damping of Beam Models Made of Dry and Wet Pine Wood,* WCTE 2008, 10th World Conference on Timber Engineering, Miyazaki, JAPAN, June 2–5, 2008.
13. Misztal B.*, Dynamic Parameters of the Free Vibrations of Various Wood Species* WCTE 2010, 11th World Conference on Timber Engineering, Riva del Garda, Trentino, Italy, June 20–24, 2010.
14. Kowal Z. *Dynamika nieważkiej belki na podłożu lepkosprężystym,* Archiwum Inżynierii Lądowej nr 1/1966, tom XII, s. 29–42.
15. Banasiak M. Ćwiczenia laboratoryjne z wytrzymałości materiałów. Praca zbiorowa. Warszawa 1985 PWN, Wydanie III zmienione.